GROWTH HORMONE RECEPTOR *(GHR)* 6Ω PSEUDOEXON ACTIVATION: A NOVEL CAUSE OF SEVERE GROWTH HORMONE INSENSITIVITY (GHI)

Emily Cottrell,[1] Avinaash Maharaj,[1] Jack Williams[1], Sumana Chatterjee,[1] Grazia Cirillo,[2] Emanuele Miraglia del Giudice,[2] Adalgisa Festa,[2] Stefania Palumbo,[2] Donatella Capalbo,[3] Mariacarolina Salerno,[4] Claudio Pignata,[4] Martin O. Savage,[1] Katharina Schilbach,[5] Martin Bidlingmaier,[5] Vivian Hwa,[6] Louise A Metherell,[1] Anna Grandone,[2] Helen L Storr[1]

[1]Centre for Endocrinology, William Harvey Research Institute: Barts and The London School of Medicine and Dentistry William Harvey Research Institute. [2]Studies of Campania Luigi Vanvitelli, Department of Woman, Child, General and Specialized Surgery. [3]Federico II University Hospital: Azienda Ospedaliera Universitaria Federico II. [4]University of Naples Federico II Department of Translational Medical Sciences: Universita degli Studi di Napoli Federico II Dipartimento di Scienze Mediche Traslazionali. [5]LMU Klinikum, Medizinische Klinik und Poliklinik IV, München. [6]Childrens Hospital Medical Center, Department of Pediatrics, University of Cincinnati College of Medicine, Cincinnati, Ohio, USA.

ORCID IDs

Emily Cottrell 0000-0001-6773-6547

Avinaash Maharaj 0000-0001-8051-3866

Jack Williams 0000-0002-1289-6671

Sumana Chatterjee 0000-0001-5273-0046

Grazia Cirillo 0000-0002-7823-972X

Emanuele Miraglia del Giudice 0000-0002-9410-5393

Adalgisa Festa 0000-0002-6747-445X

Stefania Palumbo 0000-0002-8084-9818

Donatella Capalbo 0000-0003-3312-8628

Mariacarolina Salerno 0000-0003-1310-3300

Claudio Pignata 0000-0003-1568-9843

Martin O Savage 0000-0001-7902-3376

Katharina Schilbach 0000-0002-8667-0296

Martin Bidlingmaier 0000-0002-4681-6668

Vivian Hwa 0000-0003-0517-9049

Louise A Metherell 0000-0002-0530-3524

Anna Grandone 0000-0002-6343-4768

Helen L Storr 0000-0002-9963-1931

Short title: *GHR* 6Ω pseudoexon activation in Laron syndrome

Key words: Short stature; growth hormone insensitivity; *GHR* 6Ω pseudoexon; severe primary IGF-I deficiency

Corresponding author:

Professor Helen Storr, Professor and Honorary Consultant in Paediatric Endocrinology,

Centre for Endocrinology, John Vane Science Centre, Charterhouse Square,

London EC1M 6BQ, UK.

Tel: +44 (0)20 7882 6198. Fax: +44 (0)20 7882 6197

E-mail: h.l.storr@qmul.ac.uk

Grants and fellowships: This work was supported by a Barts Charity Large Project Grant (Grant Reference Number: MRC0161) awarded to HLS, the 2018 European Society for Paediatric

Endocrinology (ESPE) Research Fellowship awarded to EC and a Sandoz Limited UK research grant 1010180 awarded to EC.

Disclosure summary: The authors have nothing to disclose.

Abstract

Context: Severe forms of Growth Hormone Insensitivity (GHI) are characterized by extreme short stature, dysmorphism and metabolic anomalies.

Objective: Identification of the genetic cause of growth failure in 3 'classical' GHI subjects.

Design: A novel intronic *GHR* variant was identified, and *in vitro* splicing assays confirmed aberrant splicing. A 6Ω pseudoexon *GHR* vector and patient fibroblast analysis assessed the consequences of the novel pseudoexon inclusion and the impact on GHR function.

Results: We identified a novel homozygous intronic *GHR* variant (g.5:42700940T>G, c.618+836T>G), 44bp downstream of the previously recognized intronic 6Ψ *GHR* pseudoexon mutation in the index patient. Two siblings also harbored the novel intronic 6Ω pseudoexon *GHR* variant in compound heterozygosity with the known *GHR* c.181C>T (R43X) mutation. *In vitro* splicing analysis confirmed inclusion of a 151bp mutant 6Ω pseudoexon not identified in wild-type constructs. Inclusion of the 6Ω pseudoexon causes a frameshift resulting in a non-functional truncated GHR lacking the transmembrane and intracellular domains. The truncated 6Ω pseudoexon protein demonstrated extracellular accumulation and diminished activation of STAT5B signaling following growth hormone stimulation.

Conclusion: Novel *GHR* 6Ω pseudoexon inclusion results in loss of GHR function consistent with a severe GHI phenotype. This represents a novel mechanism of Laron syndrome and is the first deep intronic variant identified causing severe postnatal growth failure. The 2 kindreds originate from the same town in Campania, Southern Italy, implying common ancestry. Our findings highlight the importance of studying variation in deep intronic regions as a cause of monogenic disorders.

Introduction

GH insensitivity (GHI) presents in childhood with postnatal growth failure. The severe form, 'classical GHI', is associated with extreme short stature, dysmorphic facial features and metabolic abnormalities. Biochemically, it is characterized by elevated circulating GH levels, severe IGF-I deficiency (SIGFD) and subnormal IGF-binding protein 3 (IGFBP 3) and acid labile subunit (ALS) levels (1). Classical GHI was first described in 1966 (2), and termed 'Laron syndrome' (OMIM 262500). This disorder was shown to be secondary to a defect in the growth hormone receptor gene (*GHR*) resulting in severe GH resistance (1). Since the first description, around 100 *GHR* mutations have been identified in >300 patients with significant phenotypic and biochemical variability (3).

During transcription, the entire sequence of a gene, including exons and introns, is copied to produce precursor messenger mRNA (pre-mRNA). To create a continuous coding sequence that can be translated into a protein, the introns are excised from the pre-mRNA by RNA splicing (4). The intron–exon boundaries are defined by short consensus sequences at the 5' (donor) and 3' (acceptor) splice sites that are recognized by the spliceosome. Aberrant splicing events are an established, frequent cause of monogenic human disease, but these genetic alterations are most frequently reported in the consensus sequences flanking the exons (5). Whole-genome sequencing approaches have resulted in the identification of an increasing number of pathogenic variants located deep within introns (6).

Introns frequently contain potential exonic sequences with canonical 5' and 3' sequences and flanking regions. These are termed 'pseudoexons' as they are ignored by the cellular splicing machinery and not incorporated into mature mRNA (6). Most pathological pseudoexon inclusion events originate from mutations that create a novel donor splice site and activate a pre-existing

non-canonical acceptor splice site. Less frequently, the mutation creates a novel acceptor splice site or alternatively create or disrupt splicing enhancer or silencer elements, respectively (6). Disease-causing pseudoexon inclusion was first reported in β-Thalassemia (7,8), but has subsequently been identified in patients affected by multiple disorders (6,9).

In 2001, our group described the only known intronic pseudoexon mutation to cause a growth disorder. This point mutation in intron 6 of the GH receptor (*GHR*; c.618+792A>G), was identified in four siblings with mild or 'non-classical' GHI (10). This *GHR* '6Ψ' mutation results in the inclusion of a 108 bp pseudoexon between exons 6 and 7 of the *GHR* (10), translating to an in-frame insertion of 36 amino acid residues in the extracellular domain of the GHR (10,11). In 2007, a further seven 6Ψ patients were identified (12). Recently, an in-depth analysis of the spectrum of clinical and biochemical features was reported in a total of 20 6Ψ subjects (13). Interestingly, only 50% of the 20 6Ψ patients had 'classical' GHI facial features (13). This milder, very variable phenotype (even amongst affected members of the same family) may be explained by the efficiency of splicing events that result in *GHR* transcript variability i.e. the relative abundance of different *GHR* transcripts (10,14). We report a novel *GHR* 6Ω pseudoexon resulting in severe postnatal growth failure / classical Laron syndrome.

Patients and methods

Kindred 1

The Index case (Patient 1, **Figures 1A and B**) was referred to our genetic sequencing service at 2.9 years of age with classical biochemical and phenotypic features of GH Insensitivity (GHI; 'Laron syndrome') (**Table 1**). He was the second child of unrelated non-dysmorphic Caucasian parents. He was born at 37 weeks' gestation with a normal birth weight (BW SDS -0.4). Severe postnatal growth failure was first noted at 5 months of age and by 1.7 years his height was 61 cm

(height SDS -7.4) (**Figure 1C**), he had a normal BMI 16.5 kg/m^2 (SDS -0.6) and relative macrocephaly (head circumference SDS -1.2). At presentation he had classical Laron facial features, delayed tooth eruption, small hands and feet, micropenis, bilateral undescended testes and hypoplastic scrotum. Maternal and paternal heights were -2.0 and -1.5 SDS, respectively and there was no family history of growth failure. Random serum GH was extremely elevated (38 µg/L; normal range (NR) 0-20 ng/mL). At diagnosis, he was noted to have severe deficiencies of IGF-I (<10 ng/mL; NR 13-143) and IGFBP 3 (<80 ng/ml; NR 1612-4525), ALS and GHBP levels were undetectable (<100 mU/ml and <80 pM, respectively). IGF-I levels during a 5-day IGF-I generation test (IGFGT; GH 0.033 mg/kg/day, performed according to established protocols) demonstrated an IGF-I level of <10 ng/mL at baseline and at 4 days following GH administration, indicating severe GH resistance (**Table 2**). He was diagnosed with severe GH resistance/primary IGF-I deficiency and commenced recombinant human IGF-I therapy (rhIGF-I; 120 µg/kg by subcutaneous injection twice daily) at 2.1 years of age. He had many episodes of hypoglycemia which required continuous glucose monitoring for 6 months. He developed a mild, isolated but persistent elevation of TSH (maximum 7 µU/mL; NR 0.3-4). Following commencement of rhIGF-I therapy, his height velocity improved considerably from 2.2cm/year to 8.1cm/year and has remained consistently above baseline (5.0-8.5cm/year) suggesting a good response to rhIGF-I therapy (**Figure 2**). At latest assessment aged 6 years, his height was 89 cm (-5.0 SDS) (**Figure 1C**).

Kindred 2

Patient 2 presented with severe growth failure at 9.6 years of age with a height of 83.2 cm (-9.3 SDS) and height velocity of 1.5 cm/yr (-5.2 SDS) (**Table 1 and Figure 3**). Head circumference was 45 cm (-5.7 SDS) and BMI within the normal range (-1.0 SDS). At a chronological age of 9.6 years, bone age was significantly delayed at 4.0 years. At presentation, he had small hands and feet, undescended testes and micropenis. He did not have obvious 'classical' Laron facial features

(frontal bossing or mid facial hypoplasia) but had reduced facial height (nasion to menton; -4.9 SDS) compared to head width (maximal biparietal diameter; -1.2 SDS) (15). He also suffered from mild learning difficulties, bilateral hearing loss and pubertal delay was later noted. At 40 weeks' gestation, he was born small for gestational age (SGA) with a birth weight of 2.6 kg (-2.3 SDS). The end stages of the pregnancy were complicated by pre-eclampsia. At diagnosis his basal GH levels were very elevated at 52.0 µg/mL with undetectable IGF-I and GHBP (<10 ng/mL and <80 pM, respectively) and severe deficiencies of IGFBP 3 and ALS (<80 ng/mL and <100 mU/mL, respectively). IGFGT (0.033 mg/kg/day for 7 days, as above) showed no response to GH, with baseline and peak levels of IGF-I <10 ng/mL (**Table 2**). His parents were non-consanguineous with no dysmorphic features. The father had a normal height (0.7 SDS) and his mother had short stature (-3.2 SDS). TSH levels were slightly elevated (6.8 µU/mL; NR 0.3-4.2) but FT4 1.5 ng/dl (NR 0.9-1.7) and FT3 3.0 pg/ml (NR 3.0-4.7) were consistently normal and levothyroxine therapy was never required. He commenced rhIGF-I at 12 years (120 µg/kg by subcutaneous injection twice daily) but stopped after 6 months. He recommenced rhIGF-I therapy at 18 years (height 96.2 cm, -11.8 SDS) and continued until 21 years of age (height 109.1 cm, -9.9 SDS). His height velocity improved considerably during the periods of rhIGF-I therapy but unfortunately compliance was poor and the duration of treatment was suboptimal (**Figure 2**). His final adult height at 23 years is 110 cm (-9.7 SDS) (**Figure 3**). He did not give consent for the clinical photographs at diagnosis to be included within this manuscript.

Patient 3 (**Figure 4A and B**), the younger sibling of patient 2, was also born small for gestational age (birth weight 2.1kg; -3.8 SDS) at 41 weeks gestation. At 3.4 years, he presented with a height of 67 cm (-6.9 SDS) and height velocity of 2.0 cm/yr (-4.4 SDS) (**Table 1**). His head circumference was 43.0 cm (-5.6 SDS) and BMI -4.4 SDS. At a chronological age of 3.4 years, his bone age was significantly delayed at 1.5 years. At presentation he had small hands and feet, undescended

testes, micropenis and mild papilledema. Images from early infancy showed frontal bossing **(Figure 4A)**. He also suffered from recurrent hypoglycemia, mild learning difficulties and an episode of necrotising enterocolitis. At diagnosis, baseline GH levels were elevated at 110.1 µg/L and IGFGT (0.033 mg/kg/day for 7 days, as above) showed no response to GH, with baseline and peak IGF-I levels of <10 ng/mL (**Table 2**). He had deficiencies of IGFBP 3 and ALS (274 ng/mL and <100 mU/mL, respectively). He was commenced on levothyroxine at 2 months of age due to hyperthyrotropinaemia with TSH of 13.8 µU/ml (NR 0.3-4.2). FT4 and FT3 have remained within the normal range on treatment (latest FT3 level 3.1 pg/ml; NR 3.0-4.70). He has undergone periods of rhIGF-I therapy (120 µg/kg subcutaneous injection twice daily) with variable compliance (similar to his sibling) initially commencing treatment at 5 years of age (height 70 cm, -8.1 SDS) until aged 7 years (81 cm, -7.2 SDS), restarting at 9 years (height 83 cm, -8.1 SDS) until 12 years (92 cm, -7.6 SDS). Subsequently he remained off treatment and his height at latest assessment at 14 years of age is 97.0 cm (-7.7 SDS) (**Figure 4C**). His height velocity improved during the initial period of rhIGF-I therapy, but the treatment response and outcome was likely affected by the significant compliance issues (**Figure 2**).

Biochemical assays

Biochemical assays were performed at the Endocrine Laboratory, LMU Klinikum (Munich, Germany) except for TSH, fT3 and fT4. For each assay, all samples from the same family were analysed in the same analytical run.

Serum IGF-I, GH and IGFBP 3 were measured using the IDS-iSYS platform (Immunodiagnostic Systems, Boldon, England, UK). The assays were calibrated against recombinant standards (98/574 for GH, 02/254 for IGF-I and 93/560 for IGFBP 3). Intra- and inter-assay coefficients of variability (CVs) at various concentrations ranged from 4.0–8.7% (IGF-I), 1.3–5.4% (GH) and 5.5-

12.4% (IGFBP 3). The limits of quantification are 10.0 ng/mL (IGF-I), 0.04 µg/L (GH) and 80.0 ng/mL, respectively (16-18). Serum ALS levels were measured in duplicate by sandwich immunometric assay using monoclonal antibodies directed against specific N- and C-terminal oligopeptides as previously described (19). A serum pool of healthy male volunteers was used for calibration and assigned 1000 mU/mL. Intra- and interassay CVs are <9%, the limit of quantification is 100 mU/mL, and the linear assay range is 100 to 5000 mU/mL (19). Serum GHBP concentrations were measured by an in-house, time-resolved fluorescence immunoassay (IFMA) based on monoclonal antibodies (20). The assay is standardized against recombinant non-glycosylated GHBP with concentration assigned by amino acid analysis (PRL Rehovot, Israel). Within-assay CVs were 3.4% at 312 pM and 3.4% at 2034 pM. At the same concentrations, between-assay CVs were 16.0% and 11.7%, respectively. The lower limit of quantification was 80 pM and the linear range covered concentrations between 80-4880 pM.

Ethical approval

Informed written consent for genetic research and publication of clinical details/images was obtained from patients/parents. The study was approved by the Health Research Authority, East of England - Cambridge East Research Ethics Committee (REC reference: 17/EE/0178).

Variant discovery

Genomic DNA was extracted from peripheral blood leukocytes from patient 1 and his parents using Nucleon™ BACC2 Genomic DNA Extraction Kit (GE Healthcare) in accordance with the manufacturer's instructions. Targeted whole genome sequencing was conducted using our in-house custom short stature next generation sequencing gene panel covering the entire genomic sequence (including intronic regions, 2000 bases upstream and 500 downstream) of 64 genes of

interest. These included all genes known to cause GHI and IGF-I insensitivity (*GHR, IGFI, PAPPA-2, STAT5B, IGF1R, IGFALS*) and overlapping syndromes (3M, Noonan and SRS). Probe design, preparation of libraries, capture and sequencing was performed by Otogenetics Corporation (Atlanta, US). Sequencing was performed using an Illumina HiSeq 2500 platform (paired ends 100-125, designated average coverage of 100x). H. sapiens GRCh37 (http://grch37.ensembl.org/index.html) was used as the reference genome for generating the co-ordinates of each region. Probes were designed to cover each genomic region of interest in as much detail as possible within the limitations of highly repetitive regions. For the *GHR,* coverage was ~94% (start and end coordinates 42421880 and 42722479, respectively; total size 300599bp).

Otogenetics performed data mapping, duplicate removing, snv/Indel calling, vcf annotation and generated VCF, BAM and Bam.bai files for bioinformatic analysis using Ingenuity Variant Analysis (IVA) (https://www.qiagenbioinformatics.com/products/ingenuity-variant-analysis; QIAGEN, Inc). The following filter settings were applied: call quality ≥20, read depth ≥20 and only data outside 5% of most exonically variable 100 base windows in healthy public genomes (1000 genomes, ExAC) were included. Variants predicted as loss of function as well as very rare exonic and non-coding variants of uncertain significance were also included. Common variants were filtered by excluding those with an allele frequency of ≥0.05% in the 1,000 genomes, ExAC, gnomAD and NHLBI ESP exomes.

As no exonic or canonical splice site variants were identified which could explain the phenotype, non-coding variants were explored. We identified all intronic homozygous variants with an allele frequency of ≤0.05% in the 1,000 genomes, ExAC, gnomAD and NHLBI ESP exomes. The list of variants generated were assessed using Human Splicing Finder (http://umd.be/HSF3/) which

calculated the consensus values of potential splice sites, splice enhancer and splice silencer sites. A very rare, homozygous variant in intron 6 of the *GHR* gene (42700940T>G, c.618+836T>G) was identified. This variant, altering the sequence from AGTT to AGGT, was predicted to activate an intronic cryptic donor splice site deep within intron 6 of the *GHR* (**Figure 5A**). This is a novel variant not listed in the 1,000 genomes, ExAC, gnomAD and NHLBI ESP exomes. It was assigned a CADD score <10, which is not unusual for a non-coding variant. The *GHR* sequence change was confirmed by PCR, followed by automated sequencing using primers designed to cover the affected region (GHR intron 6F (Forward) and GHR intron 6R (Reverse); sequences provided in **Supplemental Table 1** (21)) in the patient and parents. Targeted Sanger sequencing of the coding, flanking intronic and '6Ψ' regions of the *GHR* was undertaken in patients 2 and 3 and their parents (primer sequences available on request). This identified the novel intronic *GHR* (42700940T>G, c.618+836T>G) and previously reported *GHR* mutation, c.181C>T, (R43X)(22).

***In vitro* splicing assay to assess the effect of the patient variant**

An *in vitro* splicing assay was performed using the Exontrap cloning vector pET01 (MoBiTec GmbH, Göttingen, Germany) containing an intronic sequence interrupted by a multiple cloning site. DNA fragments of interest from patient 1, a wild-type control (WT) and a patient with the original *GHR* pseudoexon variant (*GHR*-6Ψ; c.618+792A>G) were amplified using PCR with primers incorporating an *Xba*I restriction enzyme target site (GHR *Xba*I F (Forward) and GHR *Xba*I R (Reverse)). PCR products were assessed by Sanger sequencing, column purified using the QIAquick® PCR Purification Kit according to the manufacturer's protocol and cloned into the Exontrap vector pET01. Recombinant vector sequences were verified by Sanger sequencing using pET01 primers (ET PRIM 06 (Forward) and 07 (Reverse)). Wild-type (WT) or mutant (patient 1 and *GHR*-6Ψ) vectors were transfected into HEK293T cells using Lipofectamine 2000® (Invitrogen). RNA was extracted (QIAGEN RNeasy Plus Mini kit) 24h after transfection and cDNA generated

using High-Capacity RNA-to-cDNA™ Kit (ThermoFisher Scientific). cDNA fragments were amplified using pET01 primers ET PRIM 02 (Forward) and 03 (Reverse) and visualized on a 2% agarose gel. Primer sequences are provided in **Supplemental Table 1** (21). A detailed protocol of the mini-gene assay has previously been published (23).

Fibroblast culture

Primary fibroblast cultures were established from skin biopsies of patients 2 and 3, performed at the Department of Translational Medical Sciences, University of Naples Federico II. Cells were sub-cultured in 75cm^2 flasks at a ratio of 1:5 in DMEM high glucose (Sigma D5648) supplemented with 20% Fetal Bovine Serum (FBS) and 1% penicillin/streptomycin at 37°C in 5% CO_2. Primary dermal fibroblasts of normal human neonatal origin, (ATCC® PCS-201-010™) were used as controls.

RNA extraction, cDNA synthesis and Reverse Transcription-PCR

RNA was extracted from control and patient derived dermal fibroblasts using the RNeasy mini kit (Qiagen) according to the manufacturer's instructions. Genomic DNA removal was achieved utilizing an RNase-Free DNase Set (Qiagen, 79254). For cDNA synthesis, 1 µg of RNA (with 10mM random hexamer and nuclease free water to a volume of 15µl) was incubated at 70°C for 5 minutes. MuMLV reverse transcriptase enzyme (20U) and 5X buffer, RNase Inhibitor (25U) and dNTPs (2.5mM each) were then added to the reaction and placed on a thermo-cycler at 25°C for 10 minutes, 42°C for 90 minutes and 70°C for 15 minutes.

RT-PCR was performed using GHR cDNA Exon 4F (Forward) and GHR cDNA Exon 8R (Reverse) primers to amplify both wildtype GHR constructs and those containing the 6Ω pseudoexon insertion. RT-PCR was also performed to amplify only constructs containing the 6Ω pseudoexon

insertion using *GHR* cDNA pseudo F1 (Forward) primer, designed at the junction of the insertion of the 6Ω pseudoexon insertion, and *GHR* cDNA Exon 8R (Reverse). Primer sequences are provided in **Supplemental Table 1** (21). Thermal cycling conditions were as follows: 95°C for 5 minutes, 13x (95°C for 20 seconds, 70°C for 30 seconds (-1°C per cycle), 72°C for 60 seconds), 30x (95°C for 20 seconds, 57°C for 30 seconds, 72°C for 60 seconds) and 72°C for 5 minutes. The annealing temperature was progressively lowered from 70°C to 57°C. PCR products were run on a 2% agarose gel, visualized with LI−COR Image Studio software (LI−COR corporate, Nebraska, USA) and confirmed by Sanger sequencing.

Creation of a 6Ω pseudoexon *GHR* vector

Gibson assembly was used to recreate the novel 6Ω pseudoexon *GHR* utilising a pcDNA1 expression vector (generous gift from Professor Richard Ross) including the entire coding sequence of *GHR*. Primers were designed using Benchling assembly wizard (Benchling Biology Software 2020, https://benchling.com) and are listed in **Supplemental Table 1** (21). The 6Ω target sequence was amplified using a Phusion® High-Fidelity PCR Kit (New England Biolabs, Ipswich). PCR products were visualized by gel electrophoresis to verify sizes and *Dpn*I treated to remove methylated DNA (the original wildtype vector template). 1µl of *Dpn*I (concentration of 10units/µl) was added to each PCR tube and the sample incubated at 37°C for 3 hours. PCR product clean-up was then performed (Macherey-Nagel™ NucleoSpin™ Gel and PCR Clean-up Kit) and DNA quality/concentration was assessed using a NanoDrop spectrophotometer. NEBiocalculator calculated the volume of each product needed for optimum annealing (https://nebiocalculator.neb.com/#!/ligation). The fragments were combined in equimolar ratio to a total of 0.2pmol with 2 times the volume of NEBuilder® HiFi DNA Assembly Master Mix (New England Biolabs, Ipswich) and incubated at 50°C for 60 minutes to anneal the two fragments into a circular vector (**Supplemental Figure 1** (21)). This construct was then transformed into NEB® 5-

alpha competent *E.coli*. Single colonies were selected for mini-preparation and DNA products verified by Sanger sequencing.

Expression of constructs in mammalian cell line and growth hormone stimulation

Human embryonic kidney 293T (HEK293T) cells were seeded into 6 well plates and transfected (in duplicate) with empty vector pcDNA3.1, wild type (pcDNA1-*GHR*) and mutant 6Ω pseudoexon constructs using Lipofectamine 3000® reagent (Thermo Fisher Scientific). Cells were maintained in DMEM high glucose supplemented with 10% FBS and 1% penicillin/streptomycin (2ml/well) at 37°C in 5% CO_2 for 24 hours. Media was then discarded and cells serum-starved for a further 24 hours by the addition of reduced volume (1ml) serum-free DMEM containing 0.1% bovine serum albumin. Cell lysates and supernatants (conditioned media) were harvested at baseline and following treatment with recombinant human GH (500ng, 0.5µg/ml) (Life technology) for 20 minutes.

Western Blotting

Whole cell lysates were prepared by lysis in RIPA buffer (Sigma Aldrich) supplemented with protease and phosphatase inhibitor tablets (Roche). Protein concentrations of cell lysates were quantified using a Bradford protein assay (Bio-Rad). Cell lysates were denatured in SDS sample buffer 4X (Sigma Aldrich, MERCK) and boiled for 5 min at 95°C. Equal concentrations of protein for whole cell lysates and standard volumes of conditioned media were loaded into wells of a NuPAGE 4-12% Bis-Tris gel (Thermo-Fisher) prior to electrophoretic separation using MOPS buffer. Protein transfer to nitrocellulose membrane was achieved by electro-blotting at 15V for 50 min. The membrane was blocked with either 5% fat free milk in TBS/0.1 % Tween-20 (GHBP) or 5% BSA in TBS/0.1 % Tween-20 (STAT5, p-STAT5) and left to gently agitate for 1 h. Individual

primary antibodies were added at specific concentrations (GHBP; BioVision, Cat# 6660, RRID:AB_2892616**;** 1:1000 dilution, STAT5B; Boster Biological Technology, Cat# PA1841, RRID:AB_2892617; 1:1000 dilution, Phospho-Stat5 (Tyr694); Cell Signaling Technology Cat# 4322, RRID:AB_10544692; 1:750 dilution) and Beta-Actin (Proteintech Cat# 66009-1-Ig, RRID:AB_2687938; 1:5000 dilution) used as a housekeeping control. The membrane was incubated with primary antibody overnight at 4°C. The membrane was washed for 5 min (X3) with Tris Buffered saline-Tween20 0.1% (TBST). Secondary goat anti-rabbit (GHBP, STAT5, p-STAT5) and goat anti-mouse (Beta-Actin) antibodies were added at concentrations of 1:10000 to blocking buffer and the membrane incubated at room temperature for 60 minutes. The membrane was subsequently washed three times (5 min each) with TBST and visualized with the LI−COR Image Studio software ((LI−COR corporate, Nebraska, USA) for immuno-fluorescent detection.

Results

Characterization of the novel GHR 6Ω pseudoexon variant

The NGS short stature gene panel identified a novel homozygous variant, deep within intron 6 of the *GHR* (42700940T>G, c.618+836T>G) in patient 1. PCR amplification of the region of interest in patient 1 and his parents verified the homozygous variant in the proband and confirmed both parents were heterozygous for this genetic variant (**Figure 5A**). This variant altered the genetic sequence from AGTT to AGGT and was predicted to create an intronic cryptic donor site. This variant was novel and not listed in the ExAC or GnomAD databases. It was assigned a CADD score <10 but this is not unusual for non-coding variants. Targeted Sanger sequencing of the coding and flanking intronic regions of the *GHR* gene in patients 2 and 3 identified compound heterozygous *GHR* mutations. Both patients 2 and 3 inherited the previously published

heterozygous c.181C>T (R43X)(22,24) *GHR* variant from their father and the heterozygous c.618+836T>G novel *GHR* (6Ω) variant from their mother (**Figure 5B**).

Interestingly, the novel intronic c.618+836T>G variant is 44-bp downstream of the original *GHR* pseudoexon variant (6Ψ; c.618+792A>G) (**Figure 6A**) (10). The inclusion of this novel 151-bp *GHR* 6Ω pseudoexon is predicted to lead to a frameshift and introduction of a premature stop codon after 245 amino acids (**Figure 6B and Supplemental Figures 2 and 3** (21)). The resultant truncated protein is expected to be non-functional given it would lack both the transmembrane (encoded by exon 8; residues 265-288) and intracellular (encoded by exons 9 & 10; residues 289-638) domains of the GHR (**Figure 6C and Supplemental Figure 3** (21)).

An *in vitro* splicing assay revealed the inclusion of 151-bp in addition to the two exons of the exon trap vector confirming 6Ω pseudoexon inclusion (**Figure 6D**). Sanger sequencing of the spliced product verified this prediction confirming that the novel variant activates an intronic cryptic donor site deep within intron 6 of the *GHR.* The close proximity of a dormant splice acceptor site leads to misrecognition of this region as an exon by the spliceosome and its retention during the splicing process. Interestingly, the same dormant acceptor site is involved in the mis-splicing and inclusion of the original *GHR* 6Ψ pseudoexon (**Figure 6A**).

Patients 2 and 3 of the second kindred were compound heterozygous for the *GHR* 6Ω pseudoexon variant (c.618+836T>G) and another previously published nonsense point mutation in exon 4 of the *GHR* (c.181C>T; R43X) (22,24). The latter mutation was inherited from their father and is predicted to lead to frameshift and introduction of an early stop codon at residue 43 of the GHR.

RNA samples derived from healthy control, patients 2 and 3 and their parent's dermal fibroblasts were used to generate cDNA. RT-PCR was performed using primers using GHR cDNA Exon 4F (Forward) and GHR cDNA Exon 8R (Reverse) primers to amplify both wildtype *GHR* sequence and the 6Ω pseudoexon insertion. A 'normal' band of expected size (705 bp) was seen in all the samples, and a larger (856 bp) band was seen in patients 2, 3 and their mother, who were all heterozygous for the *GHR* 6Ω variant (c.618+836T>G) (**Figure 7A**). This larger band corresponds to the retention of the additional 151 bases 6Ω pseudoexon.

RT-PCR was also performed using primers designed to amplify only sequences containing the 6Ω pseudoexon inclusion (GHR cDNA pseudo F1 (Forward) and GHR cDNA Exon 8R (Reverse)). A 387 bp band was seen in patients 2 and 3 and their mother, all of whom are heterozygous for the *GHR* 6Ω variant (c.618+836T>G) (**Figure 7B**). Sanger sequencing confirmed the inclusion of the 151 bases *GHR* 6Ω pseudoexon in keeping with the *in vitro* findings of the MoBiTec-exontrap splicing assay. Primer sequences are provided in **Supplemental Table 1** (21).

The impact of the *GHR* 6Ω pseudoexon on GHR signaling was assessed following growth hormone stimulation (500 ng) of both wild type and 6Ω pseudoexon *GHR* constructs expressed in HEK293T cells. Tyrosine phosphorylation of STAT5B was used as a marker of intact GHR signaling. When compared to WT GHR, the 6Ω pseudoexon construct exhibited reduced phosphorylated-STAT5B following GH-stimulation (**Figure 7C**). As the truncated 6Ω pseudoexon GHR lacks both transmembrane and intracellular domains, it is unlikely to be able to anchor onto the cell surface or dimerize, significantly abrogating the activation of STAT5B and the downstream effects of growth hormone stimulation.

48 hours following transfection of the *GHR* 6Ω pseudoexon construct into HEK293T cells, the serum free conditioned media was probed using a GHBP antibody. This revealed extracellular accumulation of mutant (truncated) GHR in the *GHR* 6Ω pseudoexon transfected cells which was not present in the WT *GHR* transfected cells (**Figure 7D**). The GHR 6Ω pseudoexon protein lacks both transmembrane and intracellular domains and would result in defective anchoring to the plasma membrane. The truncated protein is secreted extracellularly and recognized by the polyclonal GHBP antibody. Interestingly, biochemical assays using serum from all 3 patients revealed undetectable GHBP (**Table 1**). The GHBP assay relies on highly specific monoclonal antibodies and the GHR 6Ω pseudoexon protein lacks an epitope crucial for one of these monoclonal antibodies.

Biochemical analysis of the kindreds 1 and 2

Biochemical analysis of patient 1 and the siblings (patients 2 and 3) revealed classical GH insensitivity with elevated basal GH levels associated with severe deficiencies of IGF-I, IGFBP 3 and ALS in keeping with their significant postnatal growth failure **(Table 2)**. IGF-I levels did not increase even after 5 and 7 days of GH stimulation (respectively) in IGFGTs. Both parents of patient 1 and the mother of patients 2 and 3 (all carriers of the novel GHR 6Ω pseudoexon variant) had normal IGF-I levels. The father of Kindred 2 (carrier of the known GHR R43X mutation) had low IGF-I levels suggesting this mutation in heterozygosity has a greater impact on IGF-I secretion than the GHR 6Ω pseudoexon variant. Patient 1's parents also had normal IGFBP 3 and ALS whereas both parents of patients 2 and 3 had insufficient IGFBP 3 and ALS consistent with the notion that IGFBP 3 and ALS levels can be regulated independently of IGF-I and have stronger GH-dependency, respectively(25). GHBP levels were normal in the parents of patient 1 and low in both parents of patients 2 and 3. The cause of this variability is unclear.

Discussion

Here, we report a novel homozygous variant c.618+836T>G in intron 6 of the *GHR*, 44bp downstream of the previously recognized pseudoexon mutation, detected by custom targeted whole gene sequencing. A minigene assay revealed inclusion of a 151bp pseudoexon due to activation of the same dormant acceptor site involved in the mis-splicing and inclusion of the original 6Ψ *GHR* pseudoexon. In contrast to the original 6Ψ *GHR* pseudoexon, incorporation of the 6Ω pseudoexon into the mature mRNA transcript leads to a frameshift and introduction of a premature termination codon after 245 amino acids resulting in a 45KDa mutant 6Ω GHR protein lacking both transmembrane and intracellular domains required to anchor the receptor in the cell membrane and intracellular signaling, respectively. We also demonstrated that the mutant 6Ω GHR leads to diminished STAT5 signaling *in vitro*. The predicted deleterious impact of the 6Ω pseudoexon inclusion is in keeping with the severe postnatal growth failure seen in all 3 patients.

Our center previously described the first *GHR* pseudoexon (6Ψ) mutation in 2001 in four siblings from a highly consanguineous Pakistani family with mild GHI (10). This homozygous point mutation (c.618+792A>G) altered the intronic sequence activating a cryptic donor splice site. Due to the presence of a nearby dormant cryptic acceptor site, this region is recognized as an exon (a 'pseudoexon') by the spliceosome and is retained during *GHR* splicing. The inclusion of this pseudoexon caused an in-frame insertion of 36 amino acid residues (lacking a stop codon) between exons 6 and 7 in the dimerization domain of the GHR. This resulted in defective trafficking (and concomitant reduced cell surface expression) rather than impaired signaling, causing a partial loss-of-function (11). As such, moderate postnatal growth failure was observed (Height SDS -3.3 to -6.0) (14). The intronic 6Ψ *GHR* mutation, 792 bases into the intron, was identified using homozygosity mapping of several polymorphic markers surrounding the *GHR*

(10). It would not be detected by conventional exonic or whole exome sequencing which only covers exons and intron-exon boundaries.

Mutations resulting in aberrant pseudoexon inclusion have been found to be disease-causing in more than 50 genes (9). In comparison to genuine exons, pseudoexons tend to have less splicing enhancer and more splicing silencer motifs (26-29). The inclusion of pseudoexons can have significant effects on the resulting protein particularly if their inclusion leads to a frameshift.

Classically, patients with severe GHI exhibit distinctive facies characterized by frontal bossing, mid-face hypoplasia and acromicria, however, marked phenotypic variability exists even within families harboring identical mutations (30). More than 90 *GHR* gene mutations have been described to date (Human Gene Mutation Database (HGMD®), of which 21 are splice site mutations. The heterozygous nonsense *GHR* mutation c.181C>T (R43X) identified in kindred 2 has been reported in Ecuadorian, Mediterranean and Russian populations (22,31,32). It is thought to have arisen independently in these diverse populations. The c.181C>T mutation occurs at a highly mutable CpG dinucleotide 'hot spot' and has been detected in patients with a variety of *GHR* haplotypes.

Consistent with the severe IGF-I deficiency, patients 1 and 3 also had ‘classical’ Laron syndrome facial features. Although patient 2 did not have the typical frontal bossing and depressed nasal bridge, he did have had reduced facial height, suggesting some phenotypic variability despite comparable biochemical abnormalities. This is in contrast to the mild to moderate growth failure seen in patients harboring the original 6Ψ pseudoexon variant which results in a less deleterious molecular defect with in-frame insertion of 36 amino acids. Interestingly, 6Ψ pseudoexon patients also have variable clinical features with lack of dysmorphic facial features in about 50%

patients (13). Our previous observation similarly indicated little correlation between facial features and the degree of short stature(13) and that linear growth may be more consistently impacted by the degree of IGF-I deficiency. Patients 2 and 3 had head circumferences (HC -5.7 and 5.6 SDS, respectively) lower than expected for classical GHI. It is established that untreated Laron syndrome patients have reduced HC (mean -3.3 SDS; range -1.8 to -5.2 SDS) which do not correlate with the severity of growth failure(33). However, the mean head circumference deficit is typically less than the mean height deficit(33). This was observed in subjects 1 (-1.2 vs -7.4 SDS) and 2 (-5.2 vs -9.3 SDS) but was less apparent in patient 3 (-5.6 vs -6.9 SDS). Patients 2 and 3 were born SGA and co-existing prenatal growth retardation may have further impacted their head size. Interestingly, patient 3 had more severe IUGR (birth weight SDS -3.8) than patient 2 (birth weight -2.3 SDS) and this may explain the differences in HC between the siblings. We did not undertake more extensive genetic testing e.g. WES in patients 2 and 3, therefore we cannot definitively rule out another underlying genetic cause for their reduced HCs.

In patient 1, rhIGF-I therapy significantly improved the height velocity from 2.2 to 8.1cm/year in the first year of treatment. This response is in keeping with the published data in which the mean height velocity amongst 21 children with severe primary IGF-I deficiency increased from 3.1 cm/year prior to treatment to 7.4 cm/year during the first year of IGF-I therapy(34). Subsequent height velocities on treatment were not as high as the initial year of IGF-I therapy but remained above baseline for up to 12 years(34). Patients 2 and 3 had some improvement in their height velocities on rhIGF-I therapy but the significant issues with compliance meant their treatment responses and outcomes were suboptimal.

Heterozygous *GHR* mutations may have a variable effect on carriers. The site of the mutation within the gene and the corresponding modification of the protein may influence the observed

phenotype of heterozygous individuals. The genetic background of the individual may also contribute to the phenotypic diversity (35,36). The relatives of severe GHI patients, exhibit a range of heights, from reduced height SDS to normal stature. The parental heights of both our pedigrees are consistent with several studies in which family members carrying heterozygous *GHR* mutations have modest reduction in height SDS (37-39). This has been most extensively studied in the large Ecuadorian cohort carrying the E180 (c.594A>G) *GHR* defect in which heterozygosity accounted for a mean height reduction of 0.55 SDS (37).

The mothers of both kindreds who carried the 6Ω pseudoexon had short stature (-2.0 and -3.2 SDS). It has been recognized that some mothers and sisters who are heterozygous for deleterious *GHR* mutations, have more significant growth failure (height <-2 SDS) compared to male carriers (39). Heterozygosity of the functionally null E180 mutation was not associated with a reduction in circulating GHBP, IGF- I, IGF- II, IGFBP 2, or IGFBP 3 levels (37,40). The parents of patient 1 and the mother of patients 2 and 3 who all carried the novel GHR 6Ω pseudoexon variant had normal IGF-I levels. Patient 1's parents (novel GHR 6Ω pseudoexon variant carriers) also had normal IGFBP 3 and ALS levels. In contrast, the father of Kindred 2 who carried the known GHR R43X mutation, had low IGF-I levels suggesting this mutation in heterozygosity has a greater impact on IGF-I secretion than either of the GHR pseudoexon variants

It is notable that all 3 patients had elevated TSH. Most patients with growth hormone insensitivity have thyroid function within the normal range (41). Furthermore, exogenous administration of IGF-I in individuals with Laron syndrome did not negatively impact thyroid function (42). However, the relationship between the GH-IGF-I system and the hypothalamic-pituitary-thyroid axis is complex and incompletely understood. GH therapy in children and adults with GH deficiency can induce a fall in serum T4 (43). This is thought to be due to the GH effect on

570 deiodination of T4 to T3, leading to higher serum T3 levels (44). It could be hypothesized that the
571 supraphysiological levels of GH seen in patients 2 and 3 are responsible for their raised TSH levels
572 due to reduced T4 feedback, but the mechanisms are not fully understood.
573
574 Both sets of parents from the 2 kindreds originate from Frattamaggiore, a town in the Campania
575 region of Southern Italy, suggesting they share common ancestry. Interestingly, the majority of
576 reported patients with GHR 6Ψ mutations are of Pakistani origin and previous work by our group
577 suggests the presence of a common ancestor (12). The E180 *GHR* splice mutation is the most
578 common mutation identified in patients with classic GHI, comprising approximately one third of
579 the known population with GHR deficiency. This mutation is concentrated in a large population
580 of individuals with Laron syndrome in Southern Ecuador and is thought to have also originated
581 from a single common ancestor (24,45).
582
583 The presence of the secreted truncated GHR protein seen following 6Ω pseudoexon inclusion *in*
584 *vitro* suggests that the novel 6Ω pseudoexon leads to a GHR protein unable to anchor to the cell
585 membrane. This truncated GHR lacking the transmembrane and intracellular domains is
586 recognized by the polyclonal GHBP antibody. Similarly, characterization of the truncating
587 p.W267**GHR* mutation, which resides early in the transmembrane domain, demonstrated
588 elevated extracellular GHBP due to defective anchoring of the mutant protein (3). The GHBP
589 assays performed in our patients utilize highly specific monoclonal GHBP capture antibodies. One
590 of these recognizes a critical epitope which resides within a large proportion of the 6Ω
591 pseudoexon inclusion region. This explains the undetectable GHBP levels in the sera of all 3
592 patients harboring the novel 6Ω pseudoexon. We know from previous analyses in Laron patients
593 that this particular antibody is also unable to bind to GHBP in patients carrying missense R161C
594 and R211G GHR mutations, the nonsense R217X mutation and the E180 and G223 splicing

595 mutations which also modify this region.

596

597 Mis-splicing events of the *GHR* gene may be due to its large intronic regions. In vertebrates,
598 splicing of genes with large introns (>250bp) may be error prone with activation of cryptic splice
599 sites compounded by an inefficient 5' splice site in the preceding exon leading to intron inclusion.
600 Both the 6Ψ and 6Ω *GHR* pseudoexon inclusion events occur in the same intronic region,
601 suggesting that intron 6 may harbor a number of cryptic splice sites. Alternatively, this cryptic
602 acceptor position may be particularly attractive, predisposing this region to be recognised as an
603 exon.

604

605 In summary, we have identified a novel intronic *GHR* 6Ω pseudoexon inclusion event which
606 results in a functionally null GHR. Three individuals from 2 kindreds harboring this mutation
607 exhibit a severe GH insensitivity phenotype and originate from the Campania region of Southern
608 Italy suggesting common ancestry. It is very likely that pseudoexons are an under-recognized
609 cause of disease. In the new genomic era, our findings highlight the importance of studying
610 variation in deep intronic regions as a cause of monogenic disorders.

611

612 **DATA AVAILABILITY**

613 The datasets generated and/or analyzed during the current study are not publicly available but
614 are available from the corresponding author on reasonable request.

615

616

617

618

619

References

1. Eshet R, Laron Z, Pertzelan A, Arnon R, Dintzman M. Defect of human growth hormone receptors in the liver of two patients with Laron-type dwarfism. Isr J Med Sci. 1984;20:8-11

2. Laron Z, Pertzelan A, Mannheimer S. Genetic pituitary dwarfism with high serum concentation of growth hormone--a new inborn error of metabolism? Isr J Med Sci. 1966;2:152-155

3. Rughani A, Zhang D, Vairamani K, Dauber A, Hwa V, Krishnan S. Severe growth failure associated with a novel heterozygous nonsense mutation in the GHR transmembrane domain leading to elevated growth hormone binding protein. Clin Endocrinol (Oxf). 2020;92:331-337

4. Berget SM. Exon recognition in vertebrate splicing. J Biol Chem. 1995;270:2411-2414

5. Nakai K, Sakamoto H. Construction of a novel database containing aberrant splicing mutations of mammalian genes. Gene. 1994;141:171-177

6. Vaz-Drago R, Custodio N, Carmo-Fonseca M. Deep intronic mutations and human disease. Hum Genet. 2017;

7. Dobkin C, Pergolizzi RG, Bahre P, Bank A. Abnormal splice in a mutant human beta-globin gene not at the site of a mutation. Proc Natl Acad Sci U S A. 1983;80:1184-1188

8. Treisman R, Orkin SH, Maniatis T. Specific transcription and RNA splicing defects in five cloned beta-thalassaemia genes. Nature. 1983;302:591-596

9. Dhir A, Buratti E. Alternative splicing: role of pseudoexons in human disease and potential therapeutic strategies. FEBS J. 2010;277:841-855

643 **10.** Metherell LA, Akker SA, Munroe PB, Rose SJ, Caulfield M, Savage MO, Chew SL, Clark AJ.
644 Pseudoexon activation as a novel mechanism for disease resulting in atypical growth-
645 hormone insensitivity. Am J Hum Genet. 2001;69:641-646
646 **11.** Maamra M, Milward A, Esfahani HZ, Abbott LP, Metherell LA, Savage MO, Clark AJ, Ross
647 RJ. A 36 residues insertion in the dimerization domain of the growth hormone receptor
648 results in defective trafficking rather than impaired signaling. J Endocrinol. 2006;188:251-
649 261
650 **12.** David A, Camacho-Hubner C, Bhangoo A, Rose SJ, Miraki-Moud F, Akker SA, Butler GE,
651 Ten S, Clayton PE, Clark AJ, Savage MO, Metherell LA. An intronic growth hormone
652 receptor mutation causing activation of a pseudoexon is associated with a broad
653 spectrum of growth hormone insensitivity phenotypes. J Clin Endocrinol Metab.
654 2007;92:655-659
655 **13.** Chatterjee S, Shapiro L, Rose SJ, Mushtaq T, Clayton PE, Ten SB, Bhangoo A, Kumbattae
656 U, Dias R, Savage MO, Metherell LA, Storr HL. Phenotypic spectrum and responses to
657 recombinant human IGF1 (rhIGF1) therapy in patients with homozygous intronic
658 pseudoexon growth hormone receptor mutation. Eur J Endocrinol. 2018;178:481-489
659 **14.** Chatterjee S, Cottrell E, Rose SJ, Mushtaq T, Maharaj AV, Williams J, Savage MO, Metherell
660 LA, Storr H. GHR gene transcript heterogeneity may explain phenotypic variability in GHR
661 pseudoexon (6Psi) patients. Endocr Connect. 2020;9(3):211-222
662 **15.** Gripp KW. Handbook of physical measurements. 3rd ed. Oxford; New York, NY: Oxford
663 University Press; 2013; 101-111.
664 **16.** Manolopoulou J, Alami Y, Petersenn S, Schopohl J, Wu Z, Strasburger CJ, Bidlingmaier M.
665 Automated 22-kD growth hormone-specific assay without interference from
666 Pegvisomant. Clin Chem. 2012;58:1446-1456

17. Bidlingmaier M, Friedrich N, Emeny RT, Spranger J, Wolthers OD, Roswall J, Korner A, Obermayer-Pietsch B, Hubener C, Dahlgren J, Frystyk J, Pfeiffer AF, Doering A, Bielohuby M, Wallaschofski H, Arafat AM. Reference intervals for insulin-like growth factor-1 (igf-i) from birth to senescence: results from a multicenter study using a new automated chemiluminescence IGF-I immunoassay conforming to recent international recommendations. J Clin Endocrinol Metab. 2014;99:1712-1721

18. Friedrich N, Wolthers OD, Arafat AM, Emeny RT, Spranger J, Roswall J, Kratzsch J, Grabe HJ, Hubener C, Pfeiffer AF, Doring A, Bielohuby M, Dahlgren J, Frystyk J, Wallaschofski H, Bidlingmaier M. Age- and sex-specific reference intervals across life span for insulin-like growth factor binding protein 3 (IGFBP-3) and the IGF-I to IGFBP-3 ratio measured by new automated chemiluminescence assays. J Clin Endocrinol Metab. 2014;99:1675-1686

19. Stadler S, Wu Z, Dressendorfer RA, Morrison KM, Khare A, Lee PD, Strasburger CJ. Monoclonal anti-acid-labile subunit oligopeptide antibodies and their use in a two-site immunoassay for ALS measurement in humans. J Immunol Methods. 2001;252:73-82

20. Rowlinson SW, Behncken SN, Rowland JE, Clarkson RW, Strasburger CJ, Wu Z, Baumbach W, Waters MJ. Activation of chimeric and full-length growth hormone receptors by growth hormone receptor monoclonal antibodies. A specific conformational change may be required for full-length receptor signaling. J Biol Chem. 1998;273:5307-5314

21. Cottrell E, Maharaj A, Williams J, Chatterjee S, Cirillo G, Miraglia del Giudice E, Festa A, Palumbo S, Capalbo D, Salerno M, Pignata C, Savage MO, Schilbach K, Bidlingmaier M, Hwa V, Metherell LA, Grandone A, Storr HL. Data from: Growth Hormone Receptor (GHR) 6Ω Pseudoexon activation: a novel cause of severe Growth Hormone Insensitivity (GHI). Figshare Digital Repository. Deposited 11 March 2021. 10.6084/m9.figshare.14199779

690 **22.** Amselem S, Sobrier ML, Duquesnoy P, Rappaport R, Postel-Vinay MC, Gourmelen M,
691 Dallapiccola B, Goossens M. Recurrent nonsense mutations in the growth hormone
692 receptor from patients with Laron dwarfism. J Clin Invest. 1991;87:1098-1102
693 **23.** Maharaj A, Buonocore F, Meimaridou E, Ruiz-Babot G, Guasti L, Peng HM, Capper CP,
694 Burgos-Tirado N, Prasad R, Hughes CR, Maudhoo A, Crowne E, Cheetham TD, Brain CE,
695 Suntharalingham JP, Striglioni N, Yuksel B, Gurbuz F, Gupta S, Lindsay R, Couch R,
696 Spoudeas HA, Guran T, Johnson S, Fowler DJ, Conwell LS, McInerney-Leo AM, Drui D,
697 Cariou B, Lopez-Siguero JP, Harris M, Duncan EL, Hindmarsh PC, Auchus RJ, Donaldson
698 MD, Achermann JC, Metherell LA. Predicted Benign and Synonymous Variants in CYP11A1
699 Cause Primary Adrenal Insufficiency Through Missplicing. J Endocr Soc. 2019;3:201-221
700 **24.** Berg MA, Guevara-Aguirre J, Rosenbloom AL, Rosenfeld RG, Francke U. Mutation creating
701 a new splice site in the growth hormone receptor genes of 37 Ecuadorean patients with
702 Laron syndrome. Hum Mutat. 1992;1:24-32
703 **25.** Storr HL, Chatterjee S, Metherell LA, Foley C, Rosenfeld RG, Backeljauw PF, Dauber A,
704 Savage MO, Hwa V. Nonclassical GH Insensitivity: Characterization of Mild Abnormalities
705 of GH Action. Endocr Rev. 2019;40:476-505
706 **26.** Zhang XH, Chasin LA. Computational definition of sequence motifs governing constitutive
707 exon splicing. Genes Dev. 2004;18:1241-1250
708 **27.** Wang Z, Rolish ME, Yeo G, Tung V, Mawson M, Burge CB. Systematic identification and
709 analysis of exonic splicing silencers. Cell. 2004;119:831-845
710 **28.** Sironi M, Menozzi G, Riva L, Cagliani R, Comi GP, Bresolin N, Giorda R, Pozzoli U. Silencer
711 elements as possible inhibitors of pseudoexon splicing. Nucleic Acids Res. 2004;32:1783-
712 1791
713 **29.** Corvelo A, Eyras E. Exon creation and establishment in human genes. Genome Biol.
714 2008;9:R141

30. David A, Hwa V, Metherell LA, Netchine I, Camacho-Hubner C, Clark AJ, Rosenfeld RG, Savage MO. Evidence for a continuum of genetic, phenotypic, and biochemical abnormalities in children with growth hormone insensitivity. Endocr Rev. 2011;32:472-497

31. Berg MA, Argente J, Chernausek S, Gracia R, Guevara-Aguirre J, Hopp M, Perez-Jurado L, Rosenbloom A, Toledo SP, Francke U. Diverse growth hormone receptor gene mutations in Laron syndrome. American journal of human genetics. 1993;52:998-1005

32. Rosenbloom AL, Berg MA, Kasatkina EP, Volkova TN, Skorobogatova VF, Sokolovskaya VN, Francke U. Severe growth hormone insensitivity (Laron syndrome) due to nonsense mutation of the GH receptor in brothers from Russia. J Pediatr Endocrinol Metab. 1995;8:159-165

33. Laron Z, Iluz M, Kauli R. Head circumference in untreated and IGF-I treated patients with Laron syndrome: comparison with untreated and hGH-treated children with isolated growth hormone deficiency. Growth Horm IGF Res. 2012;22:49-52

34. Backeljauw PF, Kuntze J, Frane J, Calikoglu AS, Chernausek SD. Adult and Near-Adult Height in Patients with Severe Insulin-Like Growth Factor-I Deficiency after Long-Term Therapy with Recombinant Human Insulin-Like Growth Factor-I. . Horm Res Paediatr. 2013;80:47-56

35. Sjoberg M, Salazar T, Espinosa C, Dagnino A, Avila A, Eggers M, Cassorla F, Carvallo P, Mericq MV. Study of GH sensitivity in chilean patients with idiopathic short stature. J Clin Endocrinol Metab. 2001;86:4375-4381

36. Goddard AD, Dowd P, Chernausek S, Geffner M, Gertner J, Hintz R, Hopwood N, Kaplan S, Plotnick L, Rogol A, Rosenfield R, Saenger P, Mauras N, Hershkopf R, Angulo M, Attie K. Partial growth-hormone insensitivity: the role of growth-hormone receptor mutations in idiopathic short stature. J Pediatr. 1997;131:S51-55

740 **37.** Guevara-Aguirre J, Rosenbloom AL, Guevara-Aguirre M, Yariz K, Saavedra J, Baumbach L,
741 Shuster J. Effects of heterozygosity for the E180 splice mutation causing growth hormone
742 receptor deficiency in Ecuador on IGF-I, IGFBP-3, and stature. Growth Horm IGF Res.
743 2007;17:261-264
744 **38.** Woods KA, Dastot F, Preece MA, Clark AJ, Postel-Vinay MC, Chatelain PG, Ranke MB,
745 Rosenfeld RG, Amselem S, Savage MO. Phenotype: genotype relationships in growth
746 hormone insensitivity syndrome. J Clin Endocrinol Metab. 1997;82:3529-3535
747 **39.** Laron Z, Klinger B, Erster B, Silbergeld A. Serum GH binding protein activities identifies the
748 heterozygous carriers for Laron type dwarfism. Acta Endocrinol (Copenh). 1989;121:603-
749 608
750 **40.** Rosenbloom AL, Guevara-Aguirre J, Rosenfeld RG, Fielder PJ. Is there heterozygote
751 expression of growth hormone receptor deficiency? Acta Paediatr Suppl. 1994;399:125-
752 127
753 **41.** Laron Z. Laron syndrome (primary growth hormone resistance or insensitivity): the
754 personal experience 1958-2003. J Clin Endocrinol Metab. 2004;89:1031-1044
755 **42.** Klinger B, Ionesco A, Anin S, Laron Z. Effect of insulin-like growth factor I on the thyroid
756 axis in patients with Laron-type dwarfism and healthy subjects. Acta Endocrinol (Copenh).
757 1992;127:515-519
758 **43.** Moayeri H, Hemati A, Bidad K, Dalili H. Effects of growth hormone replacement therapy
759 on thyroid function tests in growth bhormone deficient children. Acta Medica Iranica.
760 2008;46:473-476
761 **44.** Yamauchi I, Sakane Y, Yamashita T, Hirota K, Ueda Y, Kanai Y, Yamashita Y, Kondo E, Fujii
762 T, Taura D, Sone M, Yasoda A, Inagaki N. Effects of growth hormone on thyroid function
763 are mediated by type 2 iodothyronine deiodinase in humans. Endocrine. 2018;59:353-363

45. Goncalves FT, Fridman C, Pinto EM, Guevara-Aguirre J, Shevah O, Rosembloom AL, Hwa V, Cassorla F, Rosenfeld RG, Lins TS, Damiani D, Arnhold IJ, Laron Z, Jorge AA. The E180splice mutation in the GHR gene causing Laron syndrome: witness of a Sephardic Jewish exodus from the Iberian Peninsula to the New World? Am J Med Genet A. 2014;164A:1204-1208

FIGURE LEGENDS

Figure 1. Clinical images and growth chart of patient 1. A and B. Clinical images of patient 1 (P1; index case) aged 1.7 yr with classical Laron features of mid-facial hypoplasia, depressed nasal bridge and frontal bossing. **C.** Growth chart showing severe postnatal growth failure and response to rhIGF-I therapy

Figure 2. Height velocity charts of the patients demonstrating the benefits of rhIGF-1 therapy. **A.** Patient 1. **B.** Patient 2 and **C.** Patient 3.

Figure 3. Growth chart of patient 2. Growth chart showing severe postnatal growth failure. Periods of rhIGF-I therapy are indicated.

Figure 4. Clinical images and growth chart of patient 3. A and B. Clinical images showing patient 3 (P3; younger sibling of P2) aged 3.5 months (A) and 5.4 years (B) displaying classical Laron features of mid-facial hypoplasia, depressed nasal bridge and frontal bossing. **C**. Growth chart showing severe postnatal growth failure. Periods of IGF-I therapy are indicated.

Figure 5. Pedigrees and electropherograms for kindreds 1 and 2. Electropherograms and pedigrees showing the segregation of the c.618+836T>G *GHR* variant in affected families. **A.** Homozygous and heterozygous c.618+836T>G *GHR* variants in patient 1 (P1) and both parents, respectively. **B.** Patients 2 and 3 (P2 and 3) harboured compound heterozygous c.618+836T>G (inherited from mother) and c.181C>T (R43X) (inherited from father) *GHR* mutations.

Figure 6. Effect of novel 6Ω GHR pseudoexon c.618+836T>G variant. A. The novel 6Ω *GHR* pseudoexon c.618+836T>G variant creates an AGGT splice donor site (red) downstream of the

original *GHR* 6Ψ pseudoexon variant (c.618+792A>G) (green) which produces a CGGT splice donor site. The dormant intronic AGCC acceptor splice site involved in mis-splicing and inclusion of both pseudoexons is shown in purple. Dashed lines indicate interrupted intronic sequence. **B.** Schematic of the 6Ψ and novel 6Ω *GHR* pseudoexons inclusion events into the mRNA. **C.** Schematic of the novel 6Ω *GHR* pseudoexon inclusion event and predicted GHR protein compared to wildtype sequence. The 6Ω pseudoexon inclusion is predicted to cause a frameshift and result in premature truncation of the GHR lacking both transmembrane (TM) and intracellular domains. **D.** Gel electrophoresis of cDNA splicing products following the splicing assay using an exon trap vector (MoBiTec-exontrap cloning vector pET01). EV, empty vector, pET01 alone; WT-*GHR*, pET01 with 600bp of wildtype *GHR* intron 6 sequence inserted; patient 1, pET01 with 600bp of patient 1 intron 6 sequence inserted (including the c.618+836T>G variant). *GHR*-6Ψ, pET01 with 600bp sequence from a patient with the original *GHR* pseudoexon (6Ψ) c.618+792A>G variant. The spliced products were amplified by PCR and visualized on a 2% agarose gel. Lanes 1 and 2: A 250bp band is seen in empty vector and WT sequence, as expected, representing the two exons of the exon trap vector and confirming normal splicing with WT sequence (lane 2). Lane 3: A 401bp band is seen in the proband and sequencing revealed 151bp insert between the two exons of the exon trap vector (250bp) confirming novel 6Ω pseudoexon inclusion. Lane 4: A 358bp band is seen in the GHR 6Ψ patient sample and sequencing revealed a 108bp insert between the two exons (250bp) of the exon trap vector confirming the original pseudoexon inclusion, as expected. BP, base pair; WT, Wildtype; *GHR*, Growth Hormone Receptor.

Figure 7. Expression of WT and mutant transcripts in affected family members with the heterozygous c.618+836T>G *GHR* 6Ω variant. The *GHR* 6Ω pseudoexon also diminishes GH-dependent STAT5B activation and accumulates extracellularly. A. cDNA was prepared from

dermal fibroblasts derived from a healthy control and patients 2 and 3 and both parents. Schematic showing the locations of the primers (GHR cDNA Exon 4F (Forward) and GHR cDNA Exon 8R (Reverse) (blue arrows)) used to amplify the region encompassing wildtype *GHR* the *GHR* 6Ω pseudoexon insertion. A 'normal' 705 bp PCR product was seen in all the samples. An additional larger (856bp) PCR product was seen in patient 2, patient 3 and their mother, who were heterozygous for the c.618+836T>G *GHR* 6Ω variant, indicating the additional 151 bp 6Ω pseudoexon insertion. B. Schematic showing the locations of the primers (GHR cDNA pseudo F1 (Forward) and GHR cDNA Exon 8R (Reverse) (blue arrows)). The forward primer at the junction of the 6Ω pseudoexon insertion means only sequences containing the *GHR* 6Ω pseudoexon insertion are amplified. The expected 387 bp PCR product is seen in patient 2, patient 3 and their mother, all of whom are heterozygous for c.618+836T>G *GHR* variant. C. Whole cell lysates from untreated or GH-stimulated (20 min) HEK293 cells transfected with pcDNA3.1 empty vector, wild type (WT) *GHR* or 6Ω *GHR* mutant constructs. Representative immunoblots of three experiments are shown. D. Immunoblot analysis of conditioned media with anti-GHBP antibody from HEK293 cells transfected with the 6Ω *GHR* mutant construct showing extracellular accumulation of the truncated mutant 6Ω *GHR* protein. BPs, base pairs; HC, Healthy Control; P2, Patient 2; P3, Patient 3; K2M, Kindred 2 Mother; K2F Kindred 2 Father; WT, Wildtype; B Actin, Beta Actin.

Table 1. Clinical and auxological details for the patients with the novel c.618+836T>G *GHR* 6Ω pseudoexon mutation

Phenotypic details	**P1**	**P2**	**P3**
Age (years)	1.7	9.6	3.4
Height (cm) [SDS]	**61.0 [-7.4]**	**83.2 [-9.3]**	**67.0 [-6.9]**
Height velocity (cm/yr) [SDS]	**1.6 [-4.5]**	**1.5 [-5.2]**	**2.0 [-4.4]**
Weight (kg) [BMI SDS]	6.1 [-0.6]	10.7 [-1.0]	**5.5 [-4.4]**
Head circumference [SDS]	45.9cm [-1.2]	**45.0 cm [-5.7]**	**43.0 cm [-5.6]**
Bone age (years)	NK	**4.0**	**1.5**
Birth weight (kg) (gestation) [SDS]	2.8 (37/40) [-0.4]	**2.6 (40/40) [-2.3]**	**2.1 (41/40) [-3.8]**
Other phenotypic details	Small hands and feet Undescended testes Hypoplastic scrotum Micropenis Delayed tooth eruption	Small hands and feet Undescended testes Micropenis Mild learning difficulties Bilateral hearing loss Pubertal delay	Small hands and feet Undescended testes Micropenis Mild learning difficulties Recurrent hypoglycemia Mild papilloedema Necrotising enterocolitis

P1, patient 1; P2, patient 2; P3, patient 3; SDS, Standard Deviation Score; NK, not known; SDS, Standard Deviation Scores.

869 **Table 2. Biochemical details of the patients with the novel c.618+836T>G *GHR* 6Ω pseudoexon mutation and their parents**

	Kindred 1			Kindred 2			
	Patient 1 (P1)	**P1 Mother**	**P1 Father**	**Patient 2 (P2)**	**Patient 3 (P3)**	**P2/3 Mother**	**P2/3 Father**
Age at presentation (years)	1.7	42.5	42.1	9.6	3.4	42.5	42.9
Height SDS	**-7.4**	**-2.0**	-1.5	**-9.3**	**-6.9**	**-3.2**	-0.7
Basal GH (µg/L)	**38.0**	ND	ND	**52.0**	**110.0**	0.21	5.23
IGF-I (ng/mL) [SDS]	**<10 [-2.6]***	165 [+0.9]	244 [+2.7]	**<10 [-3.4]**	**<10 [-2.7]**	70 [-1.7]	**45 [-2.8]**
IGFGT: Basal; Peak IGF-I (ng/ml)	**<10; <10**	ND	ND	**<10; <10**	**<10; <10**	ND	ND
IGFBP 3 (ng/mL) [SDS]	**<80 [-4.1]***	3333 [-1.1]	3897 [-0.1]	**<80 [-4.6]**	**274 [-3.8]**	**1603 [-3.0]**	**1700 [-2.9]**
ALS (mU/mL) [SDS]	**<100 [-2.6]***	620 [0.1]	594 [-0.1]	**<100 [-4.3]**	**<100 [-2.6]**	**183 [-2.6]**	**184 [-2.6]**
GHBP (pM) [SDS]	**<80***	1345 [-1.0]	701 [-1.8]	**<80**	**<80**	**247 [-2.4]**	**111 [-2.6]**
TSH (µU/mL) [NR]	**7.0 [0.3-4.0]**	ND	ND	**6.8 [0.3-4.2]**	**13.8 [0.3-4.2]**	ND	ND

870 ND, not done; NR, normal range; SDS, Standard Deviation Scores calculated based on the normal ranges for age and sex; IGFGT, IGF-I generation tests (following
871 established protocols using GH 0.033 mg/kg/day for 5 days (patient 1) and 7 days (patients 2 and 3)). *Samples obtained at 3.2 years of age.
872

Figure 1

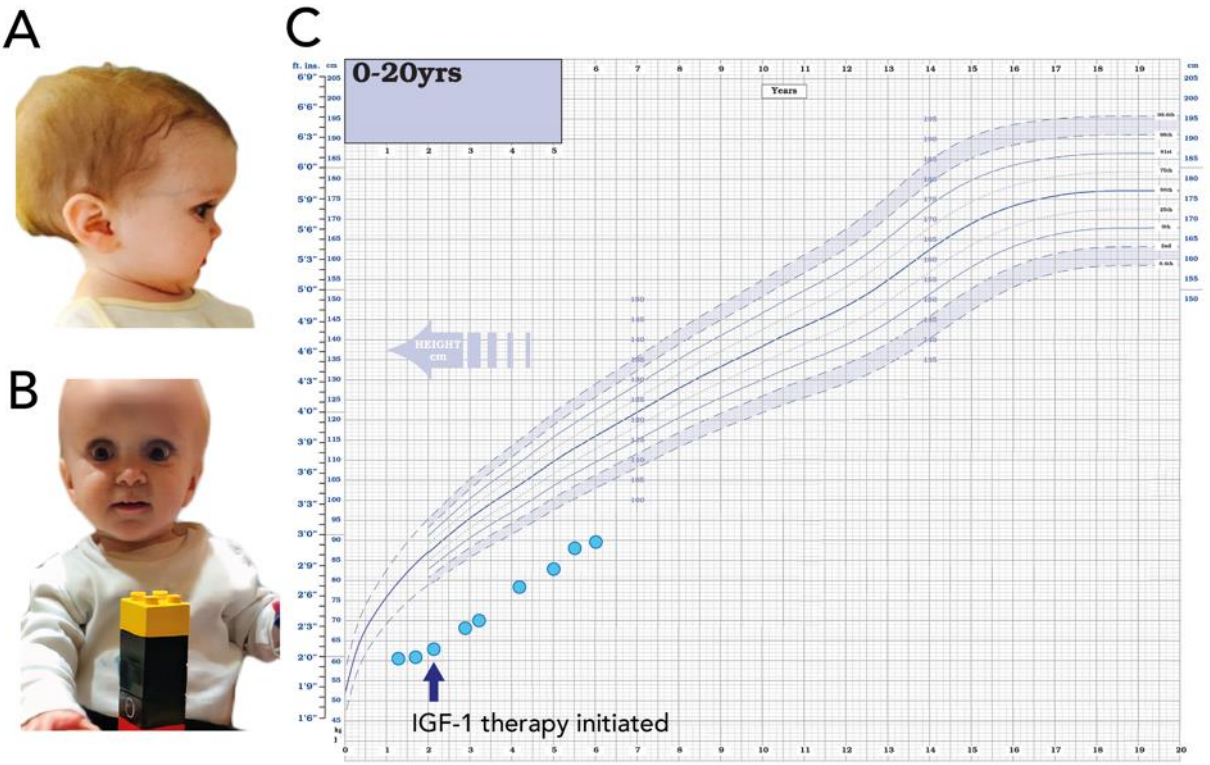

Figure 2

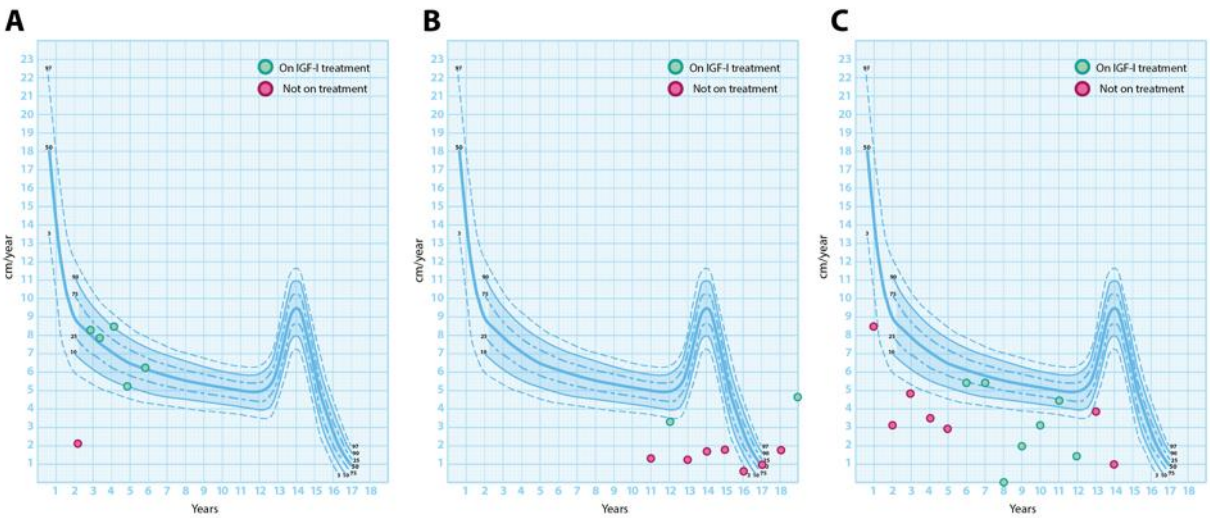

Figure 3

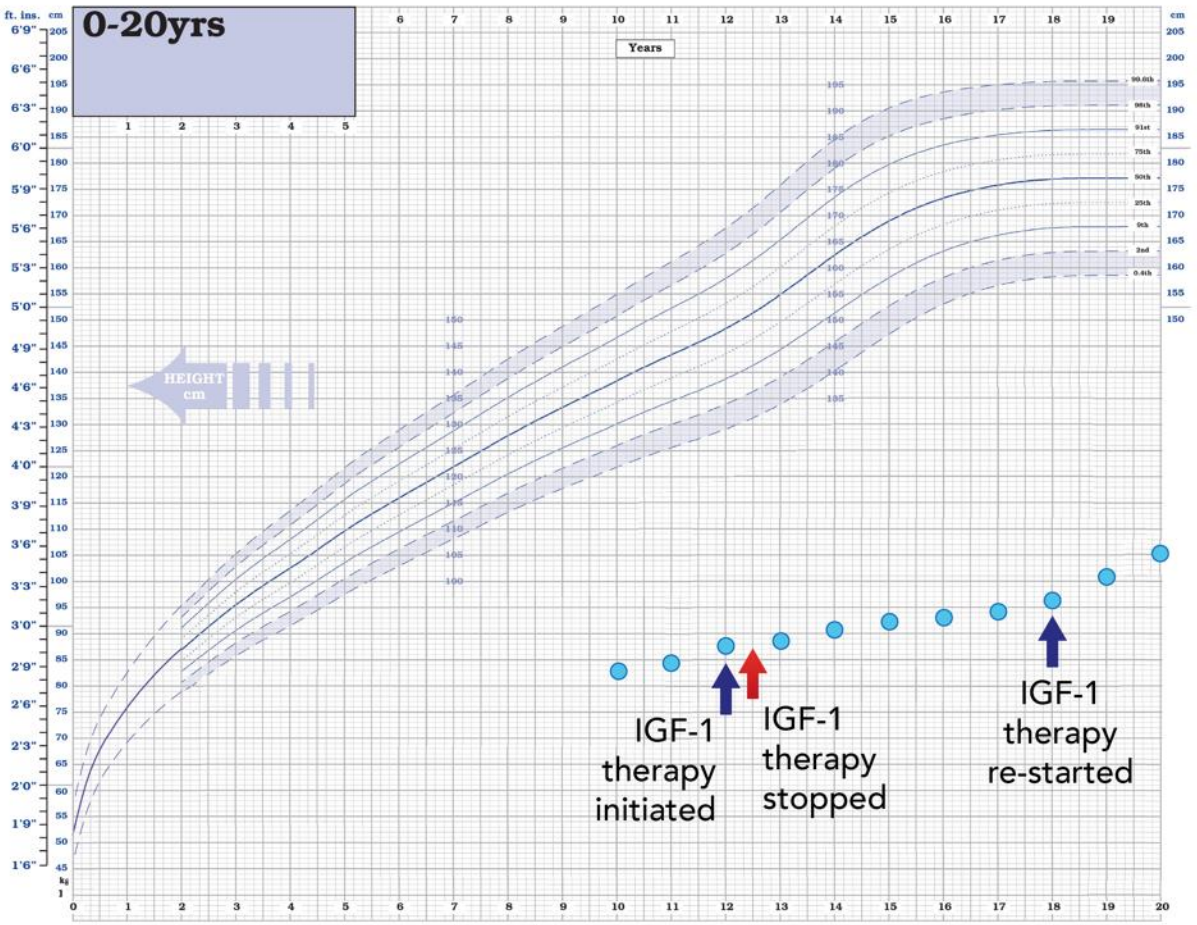
0-20yrs
Years
HEIGHT
cm
IGF-1
therapy
initiated
IGF-1
therapy
stopped
IGF-1
therapy
re-started

Figure 4

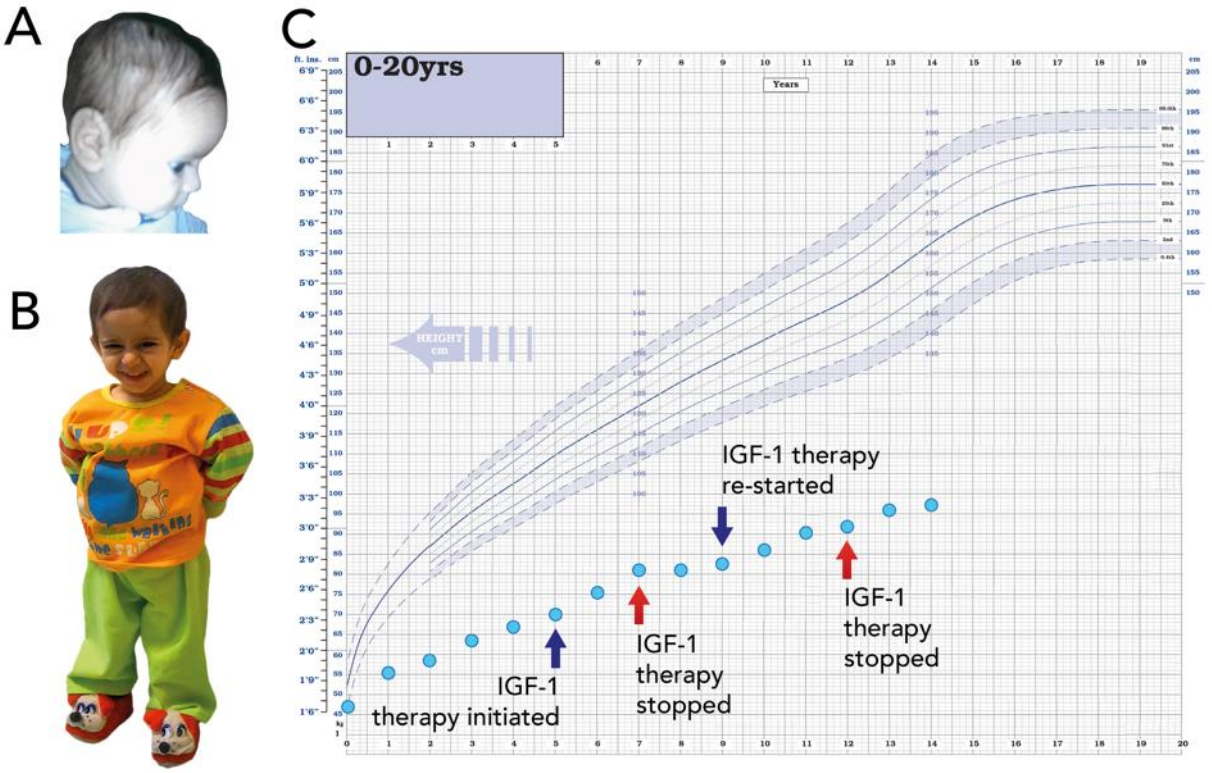
A
B
C
0-20yrs
Years
IGF-1 therapy initiated
IGF-1 therapy stopped
IGF-1 therapy re-started
IGF-1 therapy stopped

Figure 5

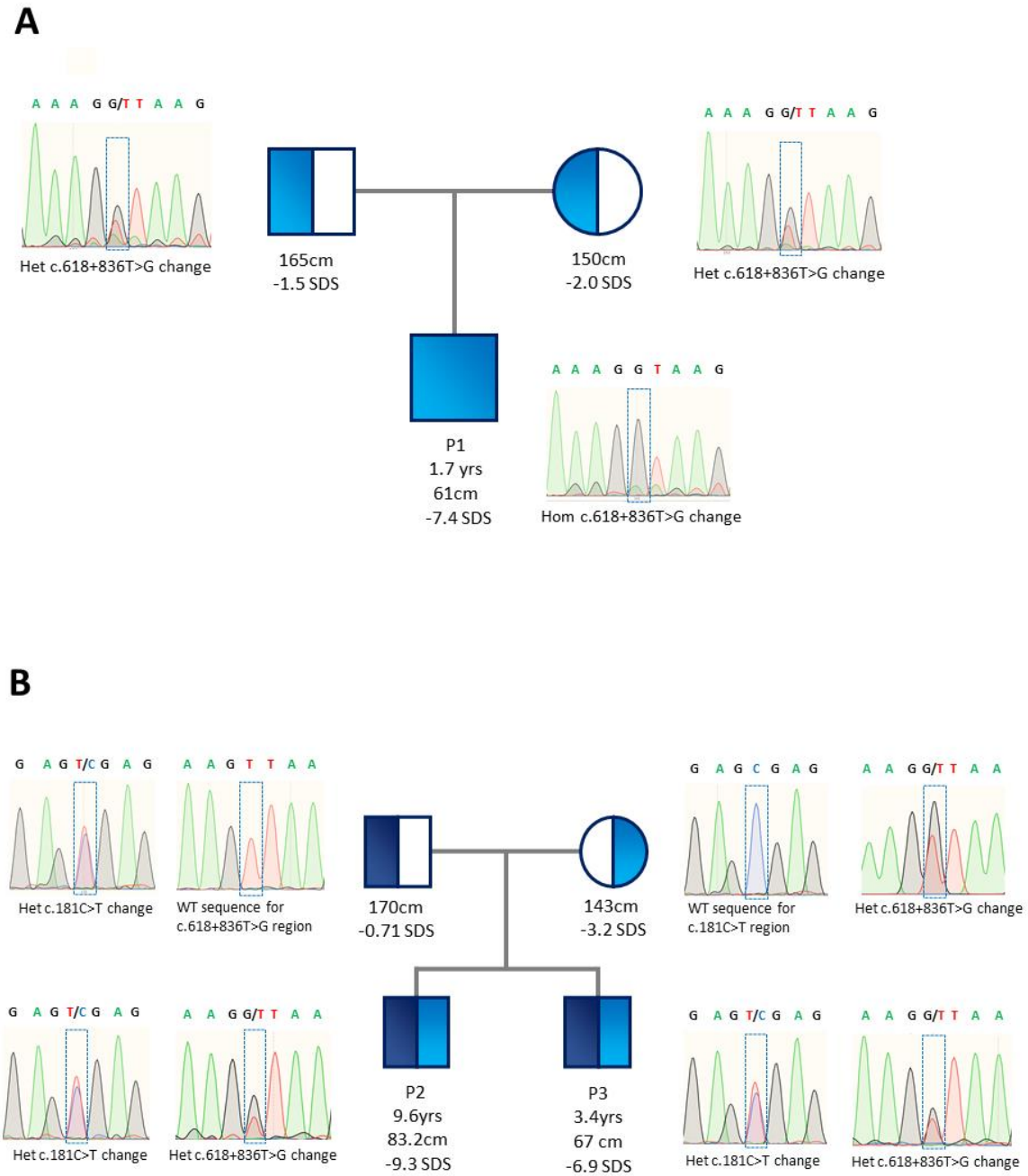
A
A A A G G/T T A A G
Het c.618+836T>G change
165cm
-1.5 SDS
150cm
-2.0 SDS
A A A G G/T T A A G
Het c.618+836T>G change
P1
1.7 yrs
61cm
-7.4 SDS
A A A G G T A A G
Hom c.618+836T>G change
B
G A G T/C G A G
Het c.181C>T change
A A G T T A A
WT sequence for
c.618+836T>G region
170cm
-0.71 SDS
143cm
-3.2 SDS
G A G C G A G
WT sequence for
c.181C>T region
A A G G/T T A A
Het c.618+836T>G change
G A G T/C G A G
Het c.181C>T change
A A G G/T T A A
Het c.618+836T>G change
P2
9.6yrs
83.2cm
-9.3 SDS
P3
3.4yrs
67 cm
-6.9 SDS
G A G T/C G A G
Het c.181C>T change
A A G G/T T A A
Het c.618+836T>G change

Figure 6

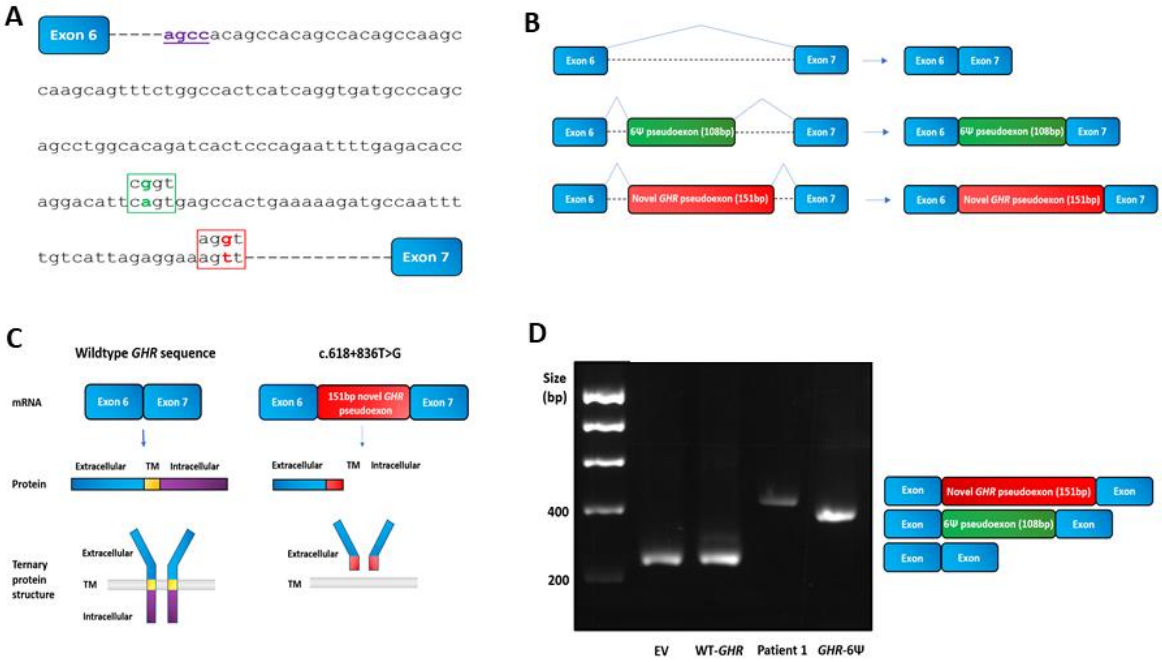

Figure 7